Product formula methods for time-dependent Schrodinger problems

1990 J. Phys. A: Math. Gen. 23 5777

(http://iopscience.iop.org/0305-4470/23/24/019)

J. Phys. A: Math. Gen. **23** (1990) 5777-5793. Printed in the UK

Product formula methods for time-dependent Schrödinger problems

J Huyghebaert† and H De Raedt‡

† Instituut voor Theoretische Fysica, University of Leuven, Celestijnenlaan 200D, B-3030 Leuven, Belgium

‡ Institute of Theoretical Physics, University of Groningen, PO Box 800, N-9700 AV Groningen, The Netherlands

Received 5 April 1990, in final form 29 August 1990

Abstract. This paper introduces a family of explicit and unconditionally stable algorithms for solving linear differential equations which contain a time-dependent Hermitian operator. Rigorous upper bounds are derived for two different 'time-ordered' approximation schemes and for errors resulting from approximating a time-ordered exponential by an ordinary exponential operator. The properties and the usefulness of the product formula algorithms are examined by applying them to the problem of Zener tunnelling. The most efficient algorithm is employed to solve the time-dependent Schrödinger equation for a wavepacket incident on a time-modulated rectangular barrier.

1. Introduction

The time development of a quantum mechanical system is governed by the time-dependent Schrödinger equation (TDSE)

$$\mathrm{i}\frac{\mathrm{d}\psi(t)}{\mathrm{d}t} = H(t)\psi(t) \tag{1.1}$$

where in general $H(t)$ is a given time-dependent linear Hermitian operator (we use units such that $\hbar = 1$). For an isolated system $H(t)$ is independent of time, i.e. the Hamiltonian, if the Schrödinger representation is chosen. In the interaction representation or in the case where the system is subject to time-dependent external forces, $H(t)$ depends explicitly on time.

The purpose of the present paper is to develop numerical algorithms to solve (1.1). Standard numerical methods, such as Runge-Kutta, are not well suited to integrate (1.1). The basic problem is that these methods do not conserve the norm of the wavefunction, an essential requirement on any method that aims at solving (1.1). Our interest in numerical methods to solve (1.1) results from the observation that, if $H(t)$ is independent of time, the Trotter formula and generalizations [1-4] of it provide a powerful mathematical setting for constructing algorithms that automatically satisfy the requirements for a proper treatment of quantum mechanical problems.

The idea behind these algorithms is to approximate the time-evolution operator $U(t, t_0) = \exp(-\mathrm{i}(t - t_0)H)$ by an ordered product [5] of unitary operators. A direct, extremely important, consequence of employing unitary approximations to the time-evolution operator is that the resulting algorithms are unconditionally stable, both from theoretical [6] as well as from numerical [4] points of view.

0305-4470/90/245777+17$03.50

To illustrate the approach assume that $H = A + B$, such that both the eigenvalue problem for A and B can be solved in closed form. The simplest Trotter formula approximation reads

$$U(t_0+\tau, t_0) = e^{-i\tau H} \simeq e^{-i\tau A}\, e^{-i\tau B} \tag{1.2}$$

which is correct up to $O(\tau)$. Obviously, the right-hand side of (1.2) is a unitary operator. A numerical algorithm that implements (1.2) would automatically preserve the norm of the wavefunction. To implement (1.2) in practice, use is made of the fact that the A and B can be diagonalized explicitly. As it is straightforward to devise much more efficient algorithms [4] by using generalizations of the Trotter formula, we strongly recommend not using (1.2) for practical purposes. It serves to illustrate the concept, nothing more.

Generalizing this concept to the case where $H(t)$ depends on time is non-trivial. The formal solution of (1.1) can be written as

$$\psi(t) = U_+(t, t_0)\psi(t_0) \tag{1.3}$$

whereby the symbol

$$U_+(t, t_0) = \exp_+\left(-i\int_{t_0}^{t} H(s)\, ds\right) \tag{1.4}$$

is defined to be the solution of

$$i\frac{\partial U_+(t, t_0)}{\partial t} = H(t)U_+(t, t_0) \qquad U_+(t_0, t_0) = 1. \tag{1.5}$$

Solving (1.5) by iteration yields the well known perturbation series

$$U_+(t, t_0) = 1 - i\int_{t_0}^{t} dt_1\, H(t_1) + i^2\int_{t_0}^{t} dt_1 \int_{t_0}^{t_1} dt_2\, H(t_1)H(t_2) + \ldots. \tag{1.6}$$

For our purposes (1.6) is useless, as truncating the series at some point would yield a non-unitary approximation to $U_+(t, t_0)$. From (1.6) it is seen that the subscript + can be interpreted as the 'time-ordering' symbol. As no use is made of (1.6) in what follows, the precise meaning of + is not important. It is sufficient to know that $U_+(t, t_0)$ is the solution of (1.5) and has the evolution property

$$U_+(t, t_0) = U_+(t, t_1)U_+(t_1, t_0) \qquad t \geqslant t_1 \geqslant t_0. \tag{1.7}$$

Starting from (1.5) and (1.7) it is straightforward to demonstrate that $U_+(t, t_0)$ shares many of the properties of exponentials [7]. The inverse of $U_+(t, t_0)$, to be denoted by $U_+^{-1}(t, t_0) \equiv U_-(t, t_0) \equiv U_+^{\dagger}(t, t_0)$, is the formal solution of

$$i\frac{\partial U_-(t, t_0)}{\partial t} = -U_-(t, t_0)H(t). \tag{1.8}$$

Other useful identities are collected in the appendix.

To set up a product formula framework we can proceed in two different manners. We may start from the formal representation of $U_+(t, t_0)$ in terms of a single exponent

$$U_+(t, t_0) = e^{X(t, t_0)} \simeq e^{\hat{X}(t, t_0)} \tag{1.9}$$

as given by Birkhoff [8], Feynman [9], Kubo [10], Fer [11], Magnus [12] and others. Note that in general $X(t, t_0)$ is an infinite series of operators, so that we have to make

some approximation and replace X by $\hat{X}$, as indicated in (1.9). The next step is to approximate $e^{\hat{X}(t,t_0)}$ by one of the generalized Trotter formulae

$$e^{\hat{X}(t,t_0)} \simeq e^{\hat{X}^{(n)}(t,t_{n-1})} e^{\hat{X}^{(n-1)}(t_{n-1},t_{n-2})} \dots e^{\hat{X}^{(1)}(t_1,t_0)}. \tag{1.10}$$

Alternatively we can approximate $U_+(t, t_0)$ by a product of similar operators

$$U_+(t, t_0) \simeq \tilde{U}_+(t, t_0) \equiv \tilde{U}_+^{(n)}(t, t_{n-1}) \tilde{U}_+^{(n-1)}(t_{n-1}, t_{n-2}) \dots \tilde{U}_+^{(1)}(t_1, t_0) \tag{1.11}$$

and then in turn approximate each of the operators by a product of exponentials

$$\tilde{U}_+^{(k)}(t_k, t_{k-1}) \simeq e^{X_1^{(k)}(t_k,t_{k-1})} e^{X_2^{(k)}(t_k,t_{k-1})} \dots e^{X_p^{(k)}(t_k,t_{k-1})}. \tag{1.12}$$

Note that if use can be made of Lie algebra properties of the operators involved, some of the steps are exact, i.e. do not involve making an approximation.

We have chosen to follow the latter route because in practical applications it is simpler and more flexible than the former. The general strategy that will be adopted is to exploit the flexibility in choosing operators and orderings such that the resulting approximant can be used in numerical work.

To illustrate the basic idea of these 'time-ordered' approximation schemes assume that $H(t) = A(t) + B(t)$. The first step is to approximate the time-evolution operator as follows

$$U_+(t, t_0) \equiv \exp_+\left(-i \int_{t_0}^{t} (A(s) + B(s))\, ds\right) \simeq \tilde{U}_+(t, t_0) \tag{1.13a}$$

$$\tilde{U}_+(t, t_0) \equiv \exp_+\left(-i \int_{t_0}^{t} A(s)\, ds\right) \exp_+\left(-i \int_{t_0}^{t} B(s)\, ds\right). \tag{1.13b}$$

Then the most simple approximation is to replace the time-ordered exponentials of the right-hand side by ordinary exponential operators,

$$U_+(t, t_0) \simeq \exp\left(-i \int_{t_0}^{t} A(s)\, ds\right) \exp\left(-i \int_{t_0}^{t} B(s)\, ds\right). \tag{1.14}$$

Often it is the case that $A(s)$ and $B(s)$ are such that the right-hand side of (1.14) can be worked out in more detail. For example, if $A(s) = A$ and $B(s) = f(s)B$ then

$$\exp_+\left(-i \int_{t_0}^{t} A(s)\, ds\right) = \exp(-iA(t - t_0)) \tag{1.15}$$

$$\exp_+\left(-i \int_{t_0}^{t} B(s)\, ds\right) = \exp\left(-iB \int_{t_0}^{t} f(s)\, ds\right). \tag{1.16}$$

If $A(t)$ and $B(t)$ can be diagonalized analytically (1.14) can be used to solve the TDSE numerically. In this paper we develop the framework to extend and examine these ideas in a systematic, rigorous manner.

The plan of the paper is as follows. In section 2 rigorous upper bounds are derived for two different 'time-ordered' approximation schemes and for the errors resulting from approximating time-ordered exponential by ordinary exponential operators. In section 3 we examine the properties and the usefulness of product formula algorithms by applying them to the standard problem of Zener tunnelling. The numerical results are compared with those obtained from the Numerov method. The conclusion is that product formula algorithms out-perform the Numerov scheme in all respects, and this in spite of the fact that the latter is particularly well suited to deal with the problem

at hand. In section 4 we use the technique developed in this paper to unravel the transmission properties of a wavepacket incident on a time dependent rectangular barrier.

2. Theory

In this section the theoretical foundation of product formula based algorithms will be given. For simplicity of notation and presentation, it will be assumed that the operator $H(t)$ can be written as a sum of two conditions $A(t)$ and $B(t)$ such that both of them are diagonalizable (for any t) not only in theory but also in practice.

As already mentioned above, the simplest scheme amounts to putting

$$U_+(t+\tau, t) = \exp_+\left(-\mathrm{i}\int_t^{t+\tau} (A(s)+B(s))\,\mathrm{d}s\right) \simeq \hat{U}_+^{(1)}(t+\tau, t) \tag{2.1}$$

$$\hat{U}_+^{(1)}(t+\tau, t) \equiv \exp_+\left(-\mathrm{i}\int_t^{t+\tau} A(s)\,\mathrm{d}s\right)\exp_+\left(-\mathrm{i}\int_t^{t+\tau} B(s)\,\mathrm{d}s\right). \tag{2.2}$$

In the appendix it is rigorously shown that the error resulting from this approximation is bounded as

$$\| U_+(t+\tau, t) - \hat{U}_+^{(1)}(t+\tau, t\| \leqslant \int_0^{\tau} \mathrm{d}x \int_0^{x} \mathrm{d}y \| [A(t+y), B(t+x)]\|. \tag{2.3}$$

In most applications $A(t)$ and $B(t)$ are smoothly varying functions of t. Then $A(t+y)$ and $B(t+x)$ can be expanded in Taylor series and (2.3) simplifies to

$$\| U_+(t+\tau, t) - \hat{U}_+^{(1)}(t+\tau, t)\| \leqslant \frac{\tau^2}{2}\| [A(t), B(t)]\| + \frac{\tau^3}{6}(\| [A'(t), B(t)]\| + 2\| [A(t), B'(t)]\|) + \mathrm{O}(\tau^4) \tag{2.4}$$

whereby $X'(t) = \mathrm{d}X(t)/\mathrm{d}t$. The next step is to replace $\exp_+(-\mathrm{i}\int_t^{t+\tau} X(s)\,\mathrm{d}s)$ by $\exp(-\mathrm{i}\int_t^{t+\tau} X(s)\,\mathrm{d}s)$, i.e. $\hat{U}_+^{(1)}(t+\tau, t)$ is approximated by

$$\tilde{U}_+^{(1)}(t+\tau, t) \equiv \exp\left(-\mathrm{i}\int_t^{t+\tau} A(s)\,\mathrm{d}s\right)\exp\left(-\mathrm{i}\int_t^{t+\tau} B(s)\,\mathrm{d}s\right). \tag{2.5}$$

Making use of the upper bound (A14), derived in the appendix, one shows that

$$\| \hat{U}_+^{(1)}(t+\tau, t) - \tilde{U}_+^{(1)}(t+\tau, t)\| \leqslant \frac{1}{2}\int_0^{\tau} \mathrm{d}x \left\| \left[A(t+x), \int_0^{\tau} \mathrm{d}y\, A(t+y)\right]\right\| + \frac{1}{2}\int_0^{\tau} \mathrm{d}x \left\| \left[B(t+x), \int_0^{\tau} \mathrm{d}y\, B(t+y)\right]\right\|. \tag{2.6}$$

Upon expanding $A(t)$ and $B(t)$ in Taylor series and combining (2.6) and (2.4) one finds

$$\| U_+(t+\tau, t) - \tilde{U}_+^{(1)}(t+\tau, t)\| \leqslant \frac{\tau^2}{2}\| [A(t), B(t)]\| + \frac{\tau^3}{6}(\| [A'(t), B(t)]\| + 2\| [A(t), B'(t)]\| + 3\| [A(t), A'(t)]\| + 3\| [B(\tau), B'(t)]\|) + \mathrm{O}(\tau^4) \tag{2.7}$$

demonstrating that the local error of this scheme is $O(\tau^2)$. As $\tilde{U}_+^{(1)}(t+\tau, t)$ is equal to $U_+(t+\tau)$ up to $O(\tau)$ we will call this approximation 'first-order method' and will indicate this by attaching the superscript '(1)'.

A more accurate approximation to $U_+(t+\tau, t)$ can be constructed from the first-order approximation by symmetrization [4], i.e.

$$\hat{U}_+^{(2)}(t+\tau, t) = \hat{U}_+^{(1)}(t+\tau, t+\tau/2)\overline{\hat{U}_+^{(1)}(t+\tau/2, t)} \tag{2.8}$$

where the bar denotes taking the transpose (not the Hermitian conjugate) of $\hat{U}_+^{(1)}(t+\tau/2, t)$. Further one approximates all the time-ordered exponentials in (2.8) by ordinary exponential operators. If $H(t) = A(t) + B(t)$ this approximation of $U(t+\tau, t)$ reads

$$\tilde{U}_+^{(2)}(t+\tau, t) = \exp\left(-\mathrm{i}\int_{t+\tau/2}^{t+\tau} A(s)\,\mathrm{d}s\right)\exp\left(-\mathrm{i}\int_t^{t+\tau} B(s)\,\mathrm{d}s\right)\exp\left(-\mathrm{i}\int_t^{t+\tau/2} A(s)\,\mathrm{d}s\right). \tag{2.9}$$

As the general expression for the error bound of this approximation is rather lengthy, we confine ourselve to the particular case $A(t) = A$ which, not entirely by accident is also frequently encountered in actual applications. As shown by (A12) the local error of this scheme is $O(\tau^3)$, hence the name 'second-order method'.

In the preceding presentation we have tacitly assumed that $A(t)$ (or A) and $B(t)$ are sufficiently simple so that they can be diagonalized by hand. In practice this is unlikely to be the case. What has been accomplished so far is to replace the intractable formal solution $U(t+\tau, t)$ by ordinary exponentials of operators. If necessary each of these exponents can then be computed by invoking the appropriate product formula technique for ordinary exponents [4].

In the next section, we present an illustrative example where this extra complication does not arise. We can therefore focus all our attention on the aspects related to the time-dependence of $H(t)$. In the subsequent section we treat a more complicated model where the calculation of $\exp(-\mathrm{i}tA)$ already represents a complicated problem. As in [4] it has been explained at great length how to deal with this particular problem, no discussion will be presented here.

3. Illustrative example

To illustrate how the formalism developed in the previous section can be used in practice, it is instructive to consider a model which is very simple, yet non-trivial. It is clear that a numerical problem involves at least two non-commuting 2×2 matrices. As an example we will consider the two-level Hamiltonian

$$H(t) = \alpha t\sigma^z + \Delta\sigma^x \tag{3.1}$$

where

$$\sigma^z \equiv \begin{pmatrix} 1 & 0 \\ 0 & -1 \end{pmatrix} \qquad \sigma^x \equiv \begin{pmatrix} 0 & 1 \\ 1 & 0 \end{pmatrix} \tag{3.2}$$

which is frequently used to describe Zener tunnelling [13, 14]. At any time t, the system is in a state which can be written as a linear combination of up (1, 0) and down (0, 1)

states. At a particular instant t_1 the eigenstates $(\psi_1(t_1), \psi_2(t_1))$ of $H(t_1)$ can be calculated by diagonalizing $H(t_1)$. If $\alpha \neq 0$ these eigenstates will evolve with time. This implies that in general $\psi_\mu^*(t_1)\psi_\nu(t_2) \neq 0$ if $t_1 \neq t_2$. Suppose that at t_1 the system is prepared in eigenstate '1'. Then, as time passes by, the system will make transitions from eigenstate '1' to eigenstate '2'. This transition is called Zener tunnelling.

A clear picture of what is going on in the system is obtained by solving numerically the TDSE for model (3.1) starting from a particular initial state. The outcome of such a calculation is shown in figure 1. The system is prepared in a state $\psi(t=-10)=(1,0)$ and the probabilities for finding the system in the 'up' $(|\psi_1(t)|^2)$ and the 'down' $(|\psi_2(t)|^2)$ state are monitored as a function of time.

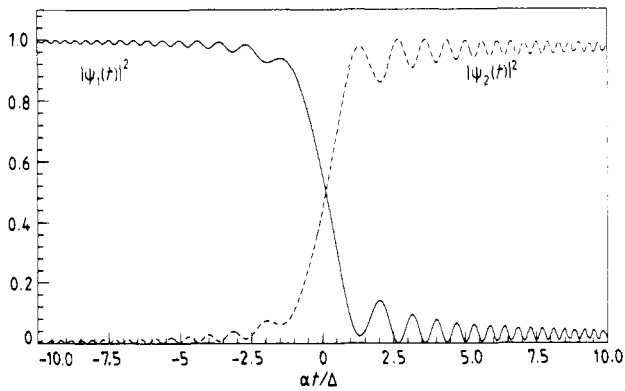

Figure 1. Probability for the Zener tunnelling system to be in the up $|\psi_1(t)|^2$ (full curve) or down $|\psi_2(t)|^2$ (broken curve) state as a function of time. In this calculation $\alpha = \Delta = \hbar = 1$.

Having discussed some of the characteristic features of model (3.1), we will now use it as an example to examine and compare various numerical methods to solve it. It is well known [14] that the TDSE for model (3.1) can be written as a second-order differential equation

$$\frac{\partial^2 \psi_2(t)}{\partial t^2} + \left(\alpha^2 t^2 + (\Delta^2 - i\alpha)\right)\psi_2(t) = 0 \tag{3.3}$$

the solutions of which are parabolic cylinder functions. The other component $\psi_1(t)$ of the wavefunction can be calculated from

$$\psi_1(t) = \frac{1}{\Delta}\left(i\frac{\partial \psi_2(t)}{\partial t} + \alpha t \psi_2(t)\right). \tag{3.4}$$

If $\psi_2(t)$ is a real-valued function, the Numerov method [15] is known to be well suited for solving (3.3) numerically. Collecting real and imaginary parts, (3.3) can be rewritten in terms of two coupled equations. Adopting the same strategy for developing the Numerov scheme as in the case of a single differential equation, one finds after some straightforward algebra

$$a_{n+1}\,\mathrm{Re}\,\varphi_{n+1} + c\,\mathrm{Im}\,\varphi_{n+1} = 2b_n\,\mathrm{Re}\,\varphi_n - a_{n-1}\,\mathrm{Re}\,\varphi_{n-1} - c(10\,\mathrm{Im}\,\varphi_n + \mathrm{Im}\,\varphi_{n-1}) \tag{3.5}$$

$$-c\,\mathrm{Re}\,\varphi_{n+1} + a_{n+1}\,\mathrm{Im}\,\varphi_{n+1} = 2b_n\,\mathrm{Re}\,\varphi_n - a_{n-1}\,\mathrm{Im}\,\varphi_{n-1} + c(10\,\mathrm{Re}\,\varphi_n + \mathrm{Re}\,\varphi_{n-1}) \tag{3.6}$$

where $\varphi_n = \psi_2(\tau n)$, $a_n = (1+\tau^2 k_n^2/12)$, $b_n = (1-5h^2k_n^2/12)$, $c = \alpha h^2/12$, $k_n^2 = \alpha^2(n\tau)^2 + \Delta^2$ and τ is the time-step used to integrate the TDSE. Also in this case the local error of the Numerov scheme is $O(\tau^6)$ [15]. Note that to start the Numerov

scheme, the state at $t=0$ (i.e. $\varphi_{n=0}$) and at $t=\tau=\tau$ (i.e. $\varphi_{n=1}$) have to be specified. It is not self-starting.

To set up a first-order product formula algorithm we put $A(t)=\alpha t\sigma^z$ and $B=\Delta\sigma^x$. The corresponding time-step operator reads

$$\tilde{U}^{(1)}(t_{k+1},t_k)=\mathrm{e}^{-\mathrm{i}\alpha\tau^2(2k+1)\sigma^z/2}\,\mathrm{e}^{-\mathrm{i}\tau\Delta\sigma^x} \tag{3.7a}$$

$$=\begin{pmatrix}\cos(\kappa\tau^2)-\mathrm{i}\sin(\kappa\tau^2) & 0\\ 0 & \cos(\kappa\tau^2)+\mathrm{i}\sin(\kappa\tau^2)\end{pmatrix}\times\begin{pmatrix}\cos(\Delta\tau) & -\mathrm{i}\sin(\Delta\tau)\\ -\mathrm{i}\sin(\Delta\tau) & \cos(\Delta\tau)\end{pmatrix} \tag{3.7b}$$

where $\kappa=\alpha(2k+1)/2$. Remark that the explicit time-dependence of $A(t)$ and $B(t)$ have been exploited to write ordinary exponents instead of 'exp$_+$'. The second line in (3.7) explicitly shows how the calculation can be implemented. In contrast to the Numerov method only the initial state has to be specified, as it should. The local error of this scheme is $O(\tau^2)$.

As explained in the previous section, a simple symmetrization procedure changes the local error from $O(\tau^2)$ to $O(\tau^3)$. From (2.9) it follows that

$$\tilde{U}^{(2)}(t_{k+1},t_k)=\mathrm{e}^{-\mathrm{i}\tau\Delta\sigma^x/2}\,\mathrm{e}^{-\mathrm{i}\alpha\tau^2(2k+1)\sigma^z/2}\,\mathrm{e}^{-\mathrm{i}\tau\Delta\sigma^x/2} \tag{3.8a}$$

$$=\begin{pmatrix}\cos(\Delta\tau/2) & -\mathrm{i}\sin(\Delta\tau/2)\\ -\mathrm{i}\sin(\Delta\tau/2) & \cos(\Delta\tau/2)\end{pmatrix}\times\begin{pmatrix}\cos(\kappa\tau^2)-\mathrm{i}\sin(\kappa\tau^2) & 0\\ 0 & \cos(\kappa\tau^2)+\mathrm{i}\sin(\kappa\tau^2)\end{pmatrix}\times\begin{pmatrix}\cos(\Delta\tau/2) & -\mathrm{i}\sin(\Delta\tau/2)\\ -\mathrm{i}\sin(\Delta\tau/2) & \cos(\Delta\tau/2)\end{pmatrix} \tag{3.8b}$$

is the desired second-order approximation to the time-step operator.

To compare the accuracy of the three different algorithms, the second-order scheme is first employed to solve the TDSE using a time-step τ small enough to obtain a solution accurate to eight significant digits ($\alpha\tau/\Delta=0.610\,351\,56\times10^{-5}$). These reference results were also used to generate $\psi_{n=1}$, required to start up the Numerov procedure. Typical results for the error on $\psi_2(t)$, i.e. $\|\psi_2(t)-\tilde{\psi}_2(t)\|$, are shown in figure 2. A first striking result is that, in spite of its $O(\tau^6)$ local error, the Numerov method is less accurate than the simplest product formula method. This is not as strange as it might seem at first sight. Note that the product formula algorithms become exact if $\alpha=0$ or $\Delta=0$ whereas for both limiting cases the Numerov method would keep generating errors. In product formula schemes, non-zero local errors result from disentangling exponents of non-commuting operators.

Figure 3 shows the RMS error $\|\psi(t)-\tilde{\psi}(t)\|$ on the full wavefunction as obtained from the first- and second-order product formula scheme. From the theoretical upper bound on the local error (see (A9) and (A12)) it is expected that the local error scales with τ^2 and τ^3 for the first- and second-order method respectively. Thus for very short times t, $\|\psi(t)-\tilde{\psi}^{(1)}(t)\|$ should be much larger as $\|\psi(t)-\tilde{\psi}^{(2)}(t)\|$, as is indeed the case (see figure 3). A more detailed analysis reveals that the local error scales with τ^{n+1} where n is the order of the product formula algorithm.

For Hamiltonians which do not explicitly depend on time, extensive numerical tests have shown that the upper bounds on the global error also correctly predicted the time dependence of the global error [4]. Apparently this is no longer the case for

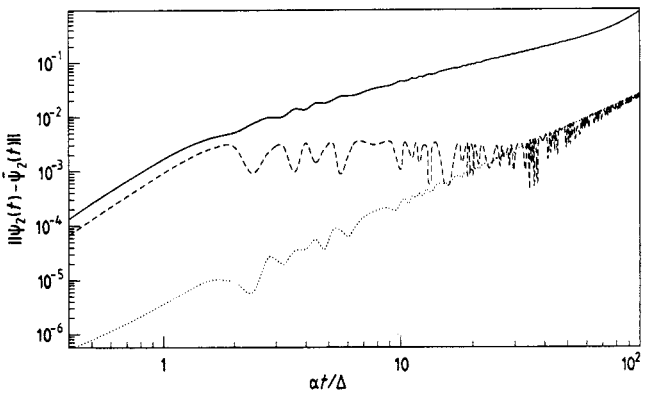

Figure 2. The error on $\psi_2(t)$, $\|\psi_2(t)-\tilde{\psi}_2(t)\|$ of the Numerov method (full curve), first- (broken curve) and second-order (dotted curve) product formula method as a function of time, for the Zener tunnelling model with $\alpha=\Delta=\hbar=1$.

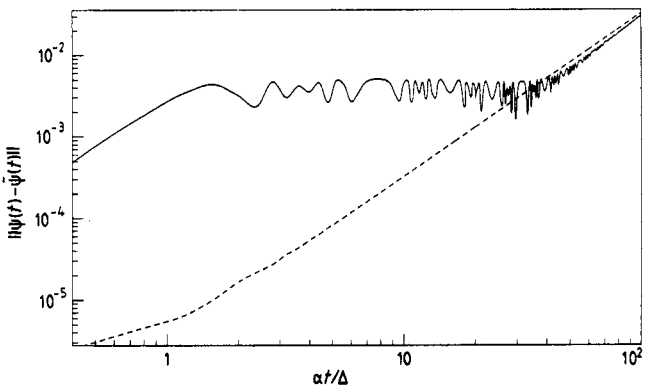

Figure 3. The RMS error $\|\psi(t)-\tilde{\psi}(t)\|$ of the first- (full curve) and second- (broken curve) order product function algorithm as a function of time for the Zener tunnelling model with $\alpha=\Delta=\hbar=1$.

the problem at hand. Figure 3 shows that for long times the error of the first- and second-order product formula algorithms are the same. Also the error of the first-order product formula algorithm is not a monotonic function of time, a feature which is very hard to explain on the basis of 'worst case' error bounds, derived by repeated use of the triangle equality. Our calculations show that the theoretical upper bounds on the global error overestimate the true global error by orders of magnitudes, and are therefore of limited practical use.

4. Time-modulated barrier

In this section we shall not focus on the properties of the product formula algorithms, but we will employ the algorithms developed in the previous chapter to study the tunnelling of a wavepacket through a time-modulated rectangular barrier. The

Hamiltonian for this system is given by

$$H(t) = -\frac{\hbar^2}{2m}\frac{\partial^2}{\partial x^2} + V_0(x) + V_1(x)\cos(\omega t) \tag{4.1}$$

whereby $V_0(x) = V_0\Theta(x)\Theta(d-x)$ is the static, rectangular potential barrier of height V_0, thickness d, and $V_1(x) = V_1\Theta(x)\Theta(d-x)$ represents the time-dependent part of the barrier which oscillates with frequency ω and amplitude V_1.

This model has already been studied by Büttiker and Landauer (BL) within perturbation theory [16]. They conclude that the tunnelling particle can absorb or emit modulation quanta $\hbar\omega$ and that the probability for these processes depends on the modulation frequency ω, the modulation height V_1 and the traversal time τ_{BL}, i.e. the time during which the particle interacts with the barrier. Further, they distinguish two frequency regimes. For a slowly oscillating potential, $\omega \ll 1/\tau_{BL}$, the particle sees, during its traversal, an effectively static barrier of height $V(t)$. If the potential varies rapidly, $\omega \gg 1/\tau_{BL}$, the particle tunnels through a time-averaged potential with effective height V_0. Büttiker and Landauer argue that the crossover between these two types of behaviour occurs at a frequency ω_{BL} where $\omega_{BL}\tau_{BL} \approx 1$ [16]. To determine the traversal time τ_{BL} of the transmitted particle one can change the modulation frequency ω until this condition is satisfied. For system (4.1) $\tau_{BL} = d\sqrt{m/2(V_0 - E_F)}$ corresponding to the time it takes for a classical free particle of mass m and kinetic energy $V_0 - E_F$ to travel the distance d.

Büttiker and Landauer have given a precise mathematical procedure which allows the identification of the crossover frequency. Calculating the intensities $t_\pm$ of the first two sidebands at $E \pm \hbar\omega$ it follows from [16, equation (7)] that

$$\ln\frac{T_+}{T_-} = 2\omega\tau_{BL} \tag{4.2}$$

or equivalently [16]

$$\frac{T_+ - T_-}{T_+ + T_-} = \tanh\,\omega\tau_{BL} \tag{4.3}$$

from which BL identify τ_{BL} as a characteristic time specifying the crossover.

The traversal time τ_{BL} is one of the possible expressions for a tunnelling time that are used at the moment [17-27]. The reason for this ambiguity is the fact that in a conservative quantum mechanical system time is not an observable and therefore it is not measurable [28]. To get around this difficulty one defines a tunnelling time by means of thought experiments [21, 29, 30]. In this chapter we are not interested in the existence of a tunnelling time itself but want to study the frequency-dependent transmission properties of model (4.1).

In our simulations [31] we solve the TDSE for Hamiltonian (4.1). At the time $t = 0$ the wavepacket has a Gaussian distribution of width σ, fixed momentum $\hbar k_F = 2\pi\hbar/\lambda_F$ and energy $E_F = \hbar^2 k_F^2/2m$. The centre of this distribution is far enough to the left of the barrier, i.e. the total probability for finding the particle in or to the right of the barrier is negligibly small ($\leq 10^{-30}$). By solving the TDSE for sufficiently long times a transmitted wavepacket will emerge. The transmitted wave is Fourier-transformed with respect to space to obtain the energy distribution (up to a change in variable: $k/k_F = \sqrt{E/E_F}$). We have chosen the model parameters d, V_0, V_1 and $\hbar^2/2m$ such that the barrier is opaque, i.e. almost completely reflecting [16]. For convenience we express

all length scales in units of λ_F, wave vectors in units of k_F, energy in units of E_F, ω in units of $E_F/\hbar$ and time in units of $\hbar/E_F$.

The accuracy of the numerical results is determined by the three following parameters: the type of discretization formulae used to approximate the second derivative in (4.1), the mesh size δ and the time-step τ used to integrate the TDSE. In practice we have used a five-point difference formula to approximate $\partial^2/\partial x^2$ and have taken 20 points per unit wavelength ($\lambda_F = 20\delta$). In this problem the time-step τ is fixed more or less by the range of ω values of interest. In practice we have worked with $\tau \leqslant \max(\omega)/100$ so that there is always a sufficient number of time-steps in one modulation period.

An important property of this model is the possibility for the particle to emit or absorb energy quanta $\hbar\omega$ as it tunnels through the barrier. Figure 4 shows us the wavevector distribution of some of the transmitted wavepackets for $\omega = 0.5$ and $\sigma = 32\lambda_F$

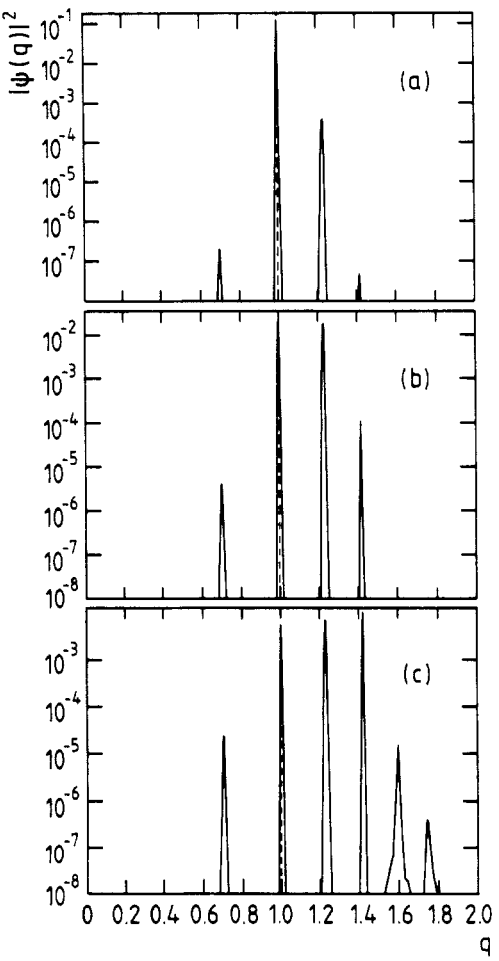

Figure 4. Wavevector distribution of transmitted wavepackets for different V_1. The incident wavepacket has width $\sigma = 32\lambda_F$, and wavevector $k = 1$. The other model parameters are: $V_0 = 1.5E_F$, $d = 5\lambda_F/3$ and $\omega = 0.5$. Peaks at $k \neq 1$ corresponds with absorption ($k > 1$) or emission ($k < 1$) of modulation quanta. (*a*) $V_1 = V_0/1000$, (*b*) $V_1 = V_0/100$, (*c*) $V_1 = V_0/10$.

for different V_1. This distribution has not only a single peak at the (incident) wavevector, $k = 1$, as in the static case, but there are different peaks at $k = \sqrt{1 + n\omega}$. These peaks corresponds with the emission or absorption of modulation quanta. The area under a peak is a measure for the probability that the corresponding emission or absorption process occurs. The number and weight of these peaks depend on the modulation amplitude V_1 and the modulation frequency ω. If $V_1/\omega \ll 1$, figure 4(a) shows that the height of these peaks is much smaller than the one at $k = 1$. Both the weight and the number of the sidebands increase with increasing V_1. For $V_1 = V_0/10$ we find that some of the peaks at $k > 1$ are more intense than the one at $k = 1$ (figure 4(c)).

Note that from figure 4 follows that the probability for absorbing quanta is always larger than for emitting the same number of quanta. Hence it follows that the energy and also the velocity of the transmitted packet will be larger than in the time-independent case. This can be seen in figure 5. This figure exemplifies the motion of the reflected and the transmitted packet. A packet transmitted through a time-modulated barrier (b) moves faster than a packet transmitted through a static barrier (a).

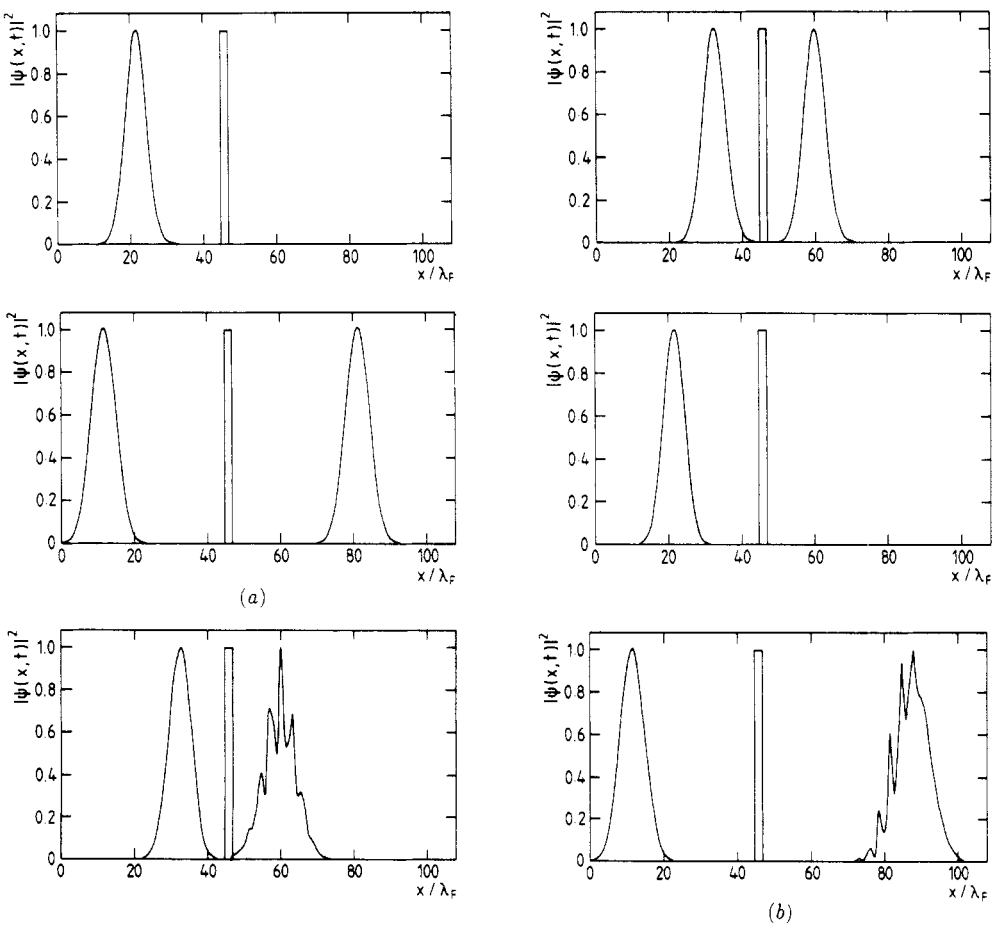

Figure 5. Probability density $|\psi(x, t)|^2$ at different times for a static (a) $V_1 = 0$ and a modulated (b) $V_1 \neq 0$ barrier. The model parameters are: $V_0 = 1.5E_F$, $V_1 = V_0/100$, $\omega = 0.5$, $d = 5\lambda_F/3$ and $\sigma = 4\lambda_F$. Note that a different scaling was used at the left and at the right of the barrier.

We now turn to the frequency dependence of the transmission coefficient

$$T(\omega, \sigma) = \lim_{t \to \infty} \int_d^{\infty} \mathrm{d}x |\psi(x, t)|^2. \tag{4.4}$$

Figure 6 shows the transmission coefficient for different values of V_1/V_0 for frequencies $0 \leqslant \omega \leqslant 1.5$. One immediately sees that in all cases the transmission coefficient of the time-modulated barrier $\omega \neq 0$ is larger than that of the static $\omega = 0$ one. As we have discussed above, the modulation leads to an increase in energy. Particles with higher energy tunnels more easily, resulting in a larger transmission coefficient. Figure 6 shows

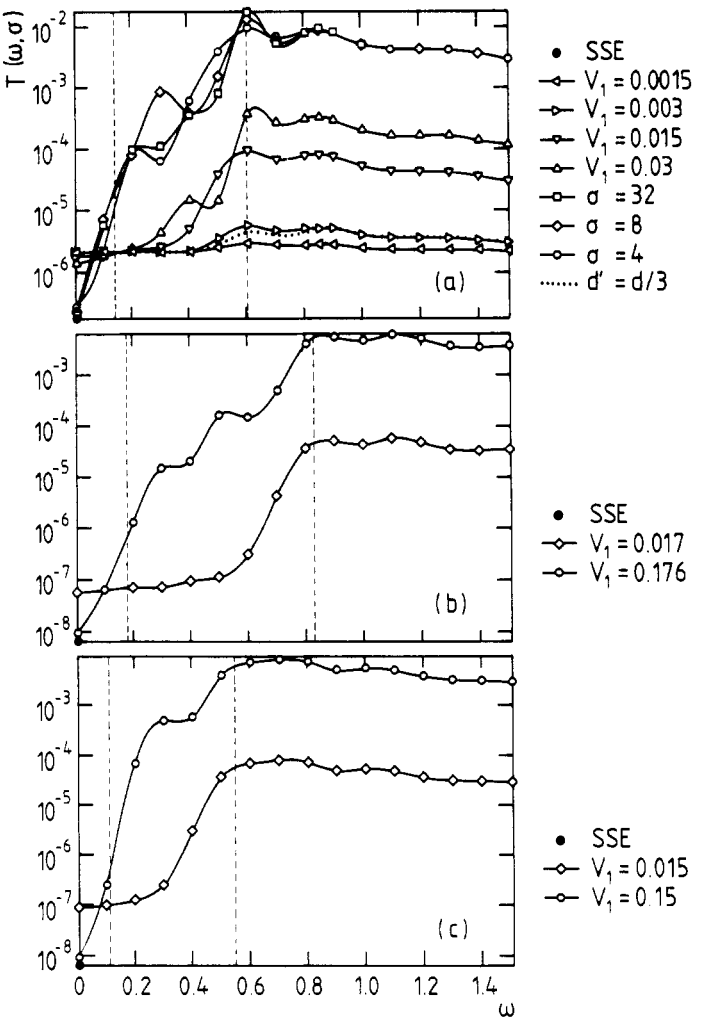

Figure 6. Transmission coefficient of a time-modulated rectangular barrier as a function of modulation frequency ω. (*a*) Model parameters are, unless specified explicitly by the legend, the same as in figure 5. The reference line closest to $\omega = 0$ corresponds to $\omega_{BL} = 1/\tau_{BL}$. The other reference line gives our estimate of ω_c. SSE denotes the rigorous solution of the stationary Schrödinger equation ($\omega = 0$). Dots represent the results for a barrier modulated over a distance $d' = d/3$ with amplitude $V_1 = 0.003 E_F$. (*b*) Same as (*a*) except $V_0 = 1.76 E_F$, and (*c*) same as (*a*) except $d = 2\lambda_F$.

that one can distinguish between two types of behaviour. If the amplitude of the modulation V_1 is large enough (e.g. $V_1 \geqslant V_0/100$) the transmission coefficient at low frequencies grows strongly by increasing the modulation frequency. At higher frequencies the transmission coefficient decreases very slowly. There exist a crossover frequency ω_c between these two regimes. From numerical simulations for barriers of various thickness and height (figure 6(b), (c)) we conclude that the position of ω_c is independent of V_1 and σ (for the values of σ considered here). From figure 6 we estimate $\omega_c(V_0 = 1.5, d = \frac{5}{3}) \approx 0.60$, $\omega_c(V_0 = 1.76, d = \frac{5}{3}) \approx 0.82$ and $\omega_c(V_0 = 1.5, d = 2) \approx 0.55$. Similar calculations (not shown) yield $\omega_c(V_0 = 1.32, d = 2) \approx 0.38$ and $\omega_c(V_0 = 1.8, d = 2) \approx 0.86$.

The physical mechanism leading to the crossover is the following. The particle can gain energy by absorbing modulation quanta. If the energy (incident plus absorbed modulation quanta) becomes larger than the barrier height, it does not have to tunnel through the barrier but goes over it. This gives rise to the plateau. In addition at certain energies there are extrema related to the resonances of the barrier. For $|V_1| \leqslant V_0/100$ the frequency at which the plateau in $T(\omega, \sigma)$ sets in is well described by the condition for the coincidence of the first-order sideband energy $1 + \omega$ with the first-order resonance energy of the static barrier, i.e.

$$\omega_R(V_0, d) = V_0 - 1 + \frac{1}{4d^2}. \tag{4.5}$$

Indeed there is almost perfect agreement between the estimates for ω_c from our simulations and the corresponding value of ω_R. For large V_1 (e.g. $V_1 = V_0/10$), higher-order peaks appear. Then it is not always possible to identify the crossover in the transmission coefficient with the resonance frequency ω_R because of the very complicated nonlinear processes.

Our simulations have led us to identify a crossover frequency ω_c. Now we want to examine if this frequency is related to the traversal time τ_{BL}, introduced by BL [16]. At the frequency $\omega_{BL} = 1/\tau_{BL}$ with ($\tau_{BL} = \pi d/\sqrt{V_0 - 1}$) there is, as indicated in figure 6, no sign of crossover between the two regimes. The product $\omega_c(V_0, d)\tau_{BL}$ has different values for barriers with different V_0 and d: $\omega_c(V_0 = 1.32, d = 2)\tau_{BL} \approx 4.3$, $\omega_c(V_0 = 1.5, d = 2)\tau_{BL} \approx 4.8$, $\omega_c(V_0 = 1.32, d = 5/3)\tau_{BL} \approx 4.4$, $\omega_c(V_0 = 1.76, d = \frac{5}{3})\tau_{BL} \approx 50$ and $\omega_c(V_0 = 1.8, d = 2)\tau_{BL} \approx 6.0$. These results strongly suggests, that the crossover frequency ω_c is not proportional to $1/\tau_{BL}$. Note, however, that

$$\omega_c \tau_{BL} \approx \omega_R \tau_{BL} = \frac{\pi}{2}\left(2\gamma + \frac{1}{2\gamma}\right) \tag{4.6}$$

whereby $\gamma = d\sqrt{V_0 - 1}$ is proportional to the tunnelling exponent of the static ($V_1 = 0$) barrier. From this it follows that only for static barriers, having the same transmission coefficient, $\omega_c(V_0, d)\tau_{BL}$ would be constant. As γ is roughly proportional to the logarithm of the transmission coefficient of the static barrier, small variations in the transmission coefficient will only cause very small changes in $\omega_c(V_0, d)\tau_{BL}$.

Changing the length of the barrier modulation might also affect the tunnelling properties. To test this we have repeated some calculations taking $V_1(x) = V_1\Theta(x)\Theta(d' - x)$ and $d' = d/3$. As illustrated in figure 6(a) there are no significant changes in the transmission coefficient. We can conclude that there is indeed a crossover between the low and high frequency behaviour, but the crossover frequency ω_c cannot be related in an obvious manner to the traversal time τ_{BL}.

To compare directly with BL we have also computed the sideband intensities $T_\pm$, as defined by BL [16], in the parameter regime where the BL analysis applies. Our

simulation results, shown in figure 7, for $\ln(T_+/T_-)$ are in perfect agreement (without fitting) with the BL prediction (4.2), for $\omega < 0.2$. Remark that BL in their derivation have made the assumption that $\omega \ll E_F$ and that $E_F = 1$ in our simulations. For $\omega \approx \omega_c$, $\ln(T_+/T_-)$ deviates from the BL prediction. Our results (figures 6 and 7) indicate that there is no crossover at a frequency proportional to $1/\tau_{BL}$, neither in the transmission coefficient nor in T_+/T_-.

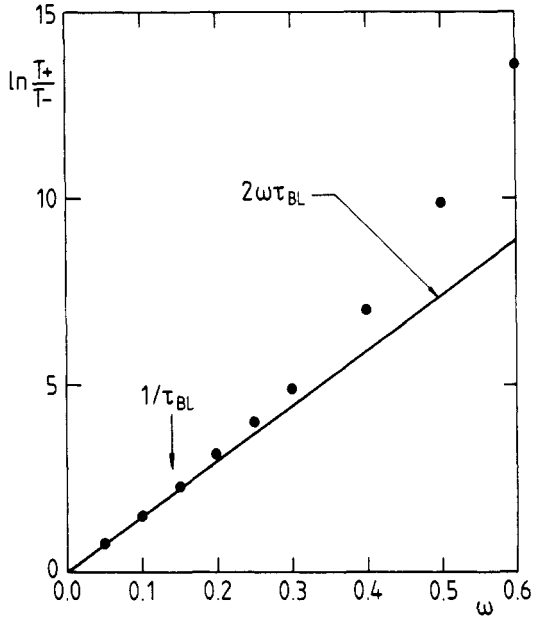

Figure 7. Ratio of the sideband intensities T_+ and T_- against frequency ω: simulation results (dots) and BL prediction (full line). The model parameters are: $V_0 = 1.5E_F$, $V_1 = V_0/1000$, $d = 5\lambda_F/3$, $\sigma = 32\lambda_F$ and $E_F = 1$.

Acknowledgments

Part of the work (section 4) was done in collaboration with N Garcia. We would like to thank R Leavens for providing us with the interpretation of ω_c in terms of ω_R, suggesting to perform simulations with $d' < d$, and for drawing our attention to a number of pertinent papers. We are grateful to P Guéret, J J Saenz, T Schneider and E Stoll for illuminating discussions. In formulating the theory we have profited from discussions with P de Vries. HDR would like to thank the University of Leuven for providing unrestricted access to their IBM 3090-300/Vf and the Belgian National Science Foundation for financial support.

Appendix A

Here we collect a number of identities used to obtain the rigorous upper bounds on which the product formula algorithms are based. In all numerical applications, the wavefunctions are vectors in a finite-dimensional Hilbert space and operators are finite

square matrices. This leads to considerable simplifications because we can dispense with all technical difficulties that would arise if we would have to work with unbounded operators.

In what follows the norm of a vector (wavefunction) is taken to be the usual one, namely $\|\phi\| \equiv \sqrt{\langle\phi|\phi\rangle}$ where $\langle\phi|\psi\rangle = \Sigma_i \phi_i^* \psi_i$ stands for the scalar product of the vectors $\phi \equiv (\ldots, \phi_i, \ldots)$ and $\psi \equiv (\ldots, \psi_i, \ldots)$. The norm of an operator X is defined by $\|X\| = \max_{\|\psi\|=1} \|X\psi\|$. If U denotes a unitary matrix, it follows immediately that $\|U\| = \|U^{-1}\| = \|U^\dagger\| = 1$.

Deriving upper bounds for the RMS error between the exact, $\psi(t)$, and the approximate, $\tilde{\psi}(t)$, wavefunction at time t requires several steps. Let $\tilde{U}_+(t, 0)$ be some approximation to the time-evolution operator $U_+(t, 0)$. Then

$$\|\psi(t) - \tilde{\psi}(t)\| = \|(U_+(t, 0) - \tilde{U}_+(t, 0))\psi(0)\| \tag{A1a}$$

$$\leq \|U_+(t, 0) - \tilde{U}_+(t, 0)\| \tag{A1b}$$

as all wavefunctions are assumed to be normalized, i.e. $\|\psi(0)\| = 1$. Next the interval $[0, t]$ is divided in m equally spaced parts. By the evolution property $U_+(t, 0) = T\prod_{k=1}^m U_+(t_k, t_{k-1})$ and $\tilde{U}_+(t, 0) = T\prod_{k=1}^m \tilde{U}_+(t_k, t_{k-1})$ whereby $t_0 = 0$, $t_m = t$ and T is the time-ordering symbol. Repeated use of the triangle equality yields

$$\|\psi(t) - \tilde{\psi}(t)\| \leq \|U_+(t, 0) - \tilde{U}_+(t, 0)\| \tag{A2a}$$

$$\leq \sum_{k=1}^{m} \|U_+(t_k, t_{k-1}) - \tilde{U}_+(t_k, t_{k-1})\|. \tag{A2b}$$

Thus the next step is to find some bound on $\|U_+(t_k, t_{k-1}) - \tilde{U}_+(t_k, t_{k-1})\|$.

Obviously it is here where the choice of a particular product formula comes in. For simplicity we only consider the case where $H(t) = A(t) + B(t)$. In the first-order scheme the approximation of the time-evolution operator $U(t_k, t_{k-1})$ is

$$\hat{U}_+^{(1)}(t_k, t_{k-1}) = \exp_+\left(-\mathrm{i}\int_{t_{k-1}}^{t_k} A(s)\,\mathrm{d}s\right)\exp_+\left(-\mathrm{i}\int_{t_{k-1}}^{t_k} B(s)\,\mathrm{d}s\right). \tag{A3}$$

Consider the operator

$$F(t_k, t_{k-1}) = \hat{U}_-^{(1)}(t_k, t_{k-1})\,U_+(t_k, t_{k-1}) - 1. \tag{A4}$$

Differentiating (A4) with respect to t_k gives after some algebra

$$\frac{\partial F(t_k, t_{k-1})}{\partial t_k} = C(t_k, t_{k-1})F(t_k, t_{k-1}) \tag{A5}$$

whereby

$$C(t_k, t_{k-1}) = \exp_-\left(+\mathrm{i}\int_{t_{k-1}}^{t_k} B(s)\,\mathrm{d}s\right)\int_{t_{k-1}}^{t_k} \mathrm{d}u\,\exp_-\left(+\mathrm{i}\int_{t_{k-1}}^{u} A(s)\,\mathrm{d}s\right)$$

$$\times[A(u), B(t_k)]\exp_+\left(-\mathrm{i}\int_{t_{k-1}}^{u} A(s)\,\mathrm{d}s\right)\exp_+\left(-\mathrm{i}\int_{t_{k-1}}^{t_k} B(s)\,\mathrm{d}s\right). \tag{A6}$$

Integrating (A5) and using $F(t_{k-1}, t_{k-1}) = 0$ yields

$$F(t_k, t_{k-1}) = \int_{t_{k-1}}^{t_k} C(v, t_{k-1})F(v, t_{k-1})\,\mathrm{d}v \tag{A7}$$

from which the upper bound

$$\|U_+(t_k, t_{k-1}) - \hat{U}_+^{(1)}(t_k, t_{k-1})\| \leq \int_{t_{k-1}}^{t_k} \mathrm{d}v \|C(v, t_{k-1})\| \tag{A8a}$$

$$\leq \int_{t_{k-1}}^{t_k} \mathrm{d}v \int_{t_{k-1}}^{v} \mathrm{d}u \|[A(u), B(v)]\| \tag{A8b}$$

follows directly. Finally this leads to

$$\|\psi(t) - \hat{\psi}^{(1)}(t)\| \leq \sum_{k=1}^{m} \int_{\tau(k-1)}^{\tau k} \mathrm{d}v \int_{\tau(k-1)}^{v} \mathrm{d}u \|[A(u), B(v)]\| \tag{A9a}$$

$$\leq \int_0^{\tau} \mathrm{d}x \int_0^{x} \mathrm{d}y \sum_{k=1}^{m} \|[A(y+\tau(k-1)), B(x+\tau(k-1))]\| \tag{A9b}$$

where we have introduced $\tau \equiv t/m$. From (A9) it is clear that if $m = 1$ the error on the wavefunctions is always $O(\tau^2)$.

In the special case where $A = A(t)$ and $B = B(t)$, (A9) reduces to

$$\|\psi(t) - \hat{\psi}^{(1)}(t)\| \leq \frac{\tau t}{2} \|[A, B]\| \tag{A10}$$

which is exactly the rigorous upper bound for the simplest Trotter formula [3, 4].

To derive the upper bound on the RMS error of the second-order scheme

$$\hat{U}_+^{(2)}(t_k, t_{k-1}) = \exp_+\left(-\mathrm{i} \int_{(t_k+t_{k-1})/2}^{t_k} A(s)\,\mathrm{d}s\right) \exp_+\left(-\mathrm{i} \int_{t_{k-1}}^{t_k} B(s)\,\mathrm{d}s\right)$$

$$\times \exp_+\left(-\mathrm{i} \int_{t_{k-1}}^{(t_k+t_{k-1})/2} A(s)\,\mathrm{d}s\right) \tag{A11a}$$

one proceeds in exactly the same way as above. Unfortunately the final expression for the upper bound in the most general case is rather lengthy. In most applications, it is possible to chose $A = A(t)$, i.e. independent of time. Then the upper bound becomes much more tractable and even useful. It reads

$$\|\psi(t) - \hat{\psi}^{(2)}(t)\| \leq \int_0^{\tau} \mathrm{d}x \int_0^{x} \mathrm{d}y \int_0^{y} \mathrm{d}z \sum_{k=1}^{m} F(z, \tau(k-1)) \tag{A12}$$

where

$$F(z, w) = \tfrac{1}{2}\|[B(z+w), [A, B(z+w)]]\| + \tfrac{1}{4}\|[A, [A, B(z+w)]]\|$$

$$+ \|[A, B''(z+w)]\| + \tfrac{3}{2}\|[A, B'(z+w)]\|$$

$$+ \|A\| \int_0^{z} \mathrm{d}u \|[B'(z+w), B(u+w)]\|$$

$$+ (\|[A, B(z+w)]\| + \|B(z+w)\|\,\|A\|) \int_0^{z} \mathrm{d}u \|[B(z+w), B(u+w)]\| \tag{A13}$$

and $B'(x) = \mathrm{d}B(x)/\mathrm{d}x$. Putting $m = 1$ in (A13) shows that $\|\psi(\tau) - \hat{\psi}^{(2)}(\tau)\| = O(\tau^3)$, which justifies the use of the term 'second-order' scheme. In the full time-independent case $B = B(t)$, (A13) reduces to the exact upper bound for the second-order Trotter formula [3, 4].

Finally it is necessary to find the RMS error that results from approximating the time-ordered operator of $U_+(t+\tau, t) = \exp_+(-\mathrm{i}\int_t^{t+\tau} H(s)\,\mathrm{d}s)$ by an ordinary exponential operator $\exp(-\mathrm{i}\int_t^{t+\tau} H(s)\,\mathrm{d}s)$. A straightforward calculation, very similar to the ones above, yields

$$\left\| \exp_+\left(-\mathrm{i}\int_t^{t+\tau} H(s)\,\mathrm{d}s\right) - \exp\left(-\mathrm{i}\int_t^{t+\tau} H(s)\,\mathrm{d}s\right) \right\| \leq \frac{1}{2}\int_0^{\tau} \mathrm{d}x \left\| \left[H(t+x)\int_0^{\tau} \mathrm{d}y\, H(t+y) \right] \right\|. \tag{A14}$$

In many practical applications is, $H(t) = f(t)H$, where $f(t)$ is a real function. For this particular case (A14) shows that no error is made if $\exp_+(-\mathrm{i}\int_t^{t+\tau} H(s)\,\mathrm{d}s)$ is replaced by $\exp(-\mathrm{i}H\int_t^{t+\tau} f(s)\,\mathrm{d}s)$.

References

[1] Suzuki M 1976 *Commun. Math. Phys.* **51** 183
[2] Suzuki M 1977 *Commun. Math. Phys.* **57** 193
[3] Suzuki M 1985 *J. Math. Phys.* **26** 601
[4] De Raedt H 1987 *Comp. Phys. Rep.* **26** 601
[5] Dollard J D and Friedman C N 1979 *Product Integration* (Reading, MA: Addison-Wesley)
[6] Smith G D 1985 *Numerical Solution of Partial Differential Equations* (Oxford: Clarendon)
[7] Kubo R 1962 *J. Phys. Soc. Japan* **17** 1100
[8] Birkhoff G 1937 *J. Math. Phys.* **16** 104
[9] Feynman R 1951 *Phys. Rev.* **84** 108
[10] Kubo R 1952 *J. Chem. Phys.* **20** 770
[11] Fer F 1958 *Bull. Classe Sci. Acad. R. Belg.* **44** 818
[12] Magnus W 1954 *Commun. Pure Appl. Math.* **7** 649
[13] Landau L D and Lifshitz E M 1958 *Quantum Mechanics* (London: Pergamon)
[14] Zener C 1932 *Proc. R. Soc. London* **137A** 696
[15] Koonin S E 1986 *Computational Physics* (Menlo Park, CA: Benjamin-Cumings)
[16] Büttiker M and Landauer R 1982 *Phys. Rev. Lett.* **49** 1739
[17] Hartman T H 1962 *J. Appl. Phys.* **33** 3427
[18] Wigner E P 1955 *Phys. Rev.* **98** 145
[19] Stevens K W 1980 *Eur. J. Phys.* **1** 98
[20] Büttiker M 1983 *Phys. Rev.* B **27** 6178
[21] Büttiker M and Landauer R 1986 *IBM J. Res. Develop.* **30** 451
[22] Collins S, Lowe D and Barker J R 1987 *J. Phys. C: Solid State Phys.* **20** 6213
[23] Jauho A P 1987 *Acta Polytechnica Scandinavia* El **58** 192
[24] Hauge E H, Falck J P and Fjeldly T A 1987 *Phys. Rev.* B **36** 4203
[25] Solovski D and Baskin L M 1987 *Phys. Rev.* A **36** 4604
[26] Falck J P and Hauge E H 1988 *Phys. Rev.* B **38** 3287
[27] Leavens C R and Aers G C 1989 *Phys. Rev.* B **39** 1202
[28] Peres A 1980 *Am. J. Phys.* **48** 552
[29] Baz' A I 1967 *Sov. J. Nucl. Phys.* **4** 182
[30] Rybachenko V F 1967 *Sov. J. Nucl. Phys.* **5** 635
[31] De Raedt H, Garcia N and Huyghebaert J *Tunnelling through time-modulated barriers: Is there a crossover frequency?* (to appear in *Solid State Commun.*)